

Electron Tunneling into Superconducting ZrN

J. Geerk, G. Linker, and R. Smithey

Institut für Nukleare Festkörperphysik, Kernforschungszentrum Karlsruhe, D-7500 Karlsruhe, Federal Republic of Germany

(Received 16 September 1986)

We have prepared tunnel junctions on superconducting ZrN thin films using the natural oxide as a tunnel barrier. In the superconducting density of states we observed the phonon-induced structures due to the acoustic and optical phonons. The tunnel data could be analyzed by the McMillan-Rowell procedure without the need to correct for proximity effects. From the resulting Eliashberg function it was concluded that the optical phonons are coupled slightly more strongly to the electrons than the acoustic phonons.

PACS numbers: 74.50.+r, 71.38.+i, 74.70.Gj

The transition-metal compounds with sodium chloride (B1) structure such as NbN, NbC, ZrN, or HfN are of considerable interest not only because of their excellent mechanical properties but also because they represent a group of superconductors with high transition temperatures T_c . For example, the carbonitrides of Nb reach T_c values above 18 K. The fundamental research on superconductivity in these compounds is mainly concerned with the electron-phonon coupling of the soft acoustic-phonon modes and that of the optical phonons which are clearly separated in energy from the acoustic part as a result of the large mass difference of the constituent atoms in the compounds. The electron-phonon coupling strength is quantitatively described by the Eliashberg function. This function is defined as the product of the phonon density of states $F(\omega)$ and an energy-dependent electron-phonon coupling function $\alpha^2(\omega)$ and describes the scattering of quasiparticles via emission and absorption of phonons. The most sensitive probe for the determination of $\alpha^2(\omega)F(\omega)$ is the method of electron tunneling. This experimental technique applies a tunnel diode to measure directly the superconducting density of states which then is used to calculate $\alpha^2(\omega)F(\omega)$ via the Eliashberg equations.

Tunneling experiments on the most attractive superconducting refractory compounds such as NbC and NbN¹⁻³ so far have suffered severely from proximity-induced deformations of the experimental data, i.e., the reduced density of states (RDOS). It is well known that such proximity effects are caused by the undesirable properties of the natural oxide of these Nb-based compounds which formed the tunnel barrier in most experimental data published so far. An artificial tunnel barrier on a refractory compound has successfully been used for tunneling spectroscopy only in the case of TiN.³ In this case an AlZr overlayer was deposited onto the freshly prepared TiN film and subsequently oxidized in air. Experimental problems with this rather complicated preparation technique have stimulated us to search for other B1 superconductors which might form a natural oxide well suited for tunneling spectroscopy. As a first

example we present in this paper tunneling measurements on ZrN, a superconductor with NaCl structure and a T_c of 9.4 K. From these measurements we were able to determine the complete Eliashberg function including the optical phonon part. We will compare our results to theoretical calculations published by Rietschel, Winter, and Reichardt.⁴

The junctions of the type ZrN/ZrN-oxide/(In or Pb) were prepared on thin films of ZrN formed by reactive magnetron sputtering. The vacuum system provided a base pressure of 10^{-8} Torr prior to deposition. Marzgrade Zr was used as a sputtering target. The films were deposited on Al₂O₃ substrates held at a temperature of 1200°C. The sputtering gas was a mixture of argon and nitrogen with $p_{Ar} = 5 \times 10^{-2}$ Torr and $p_{N_2} = 7 \times 10^{-2}$ Torr. Only gases of highest available purity (99.999%) were used. After deposition the ZrN films cooled down to room temperature in vacuum and were allowed to oxidize in laboratory air for 50 to 80 h. Then the junctions were completed by evaporation of In or Pb counter electrodes. First and second derivatives of the I - V characteristics were measured with a Kelvin bridge and a reactance network, respectively.

An oxidation of the freshly prepared films of 50 h at room temperature was necessary to yield ZrN/ZrN-oxide/In junctions with resistances between 10 and 100 Ω which are best suited for tunneling measurements. With Pb counterelectrodes the oxidation time could be much shorter (about 5 h), but the magnetic field of about 0.2 T, applied for full suppression of the superconductivity in the Pb electrode, also reduced the energy gap of the ZrN film. Therefore In counterelectrodes were used.

We have made seven runs with optimized preparation parameters and fabricated 24 high-quality tunnel junctions. The dI/dV trace at low voltages in the region of the energy gap of one of the best junctions is shown in Fig. 1. The trace was measured at 1.2 K with both electrodes in the superconducting state. We observe very sharp peaks at the voltage of ± 2 mV corresponding to the sum of the energy gaps of the two electrodes

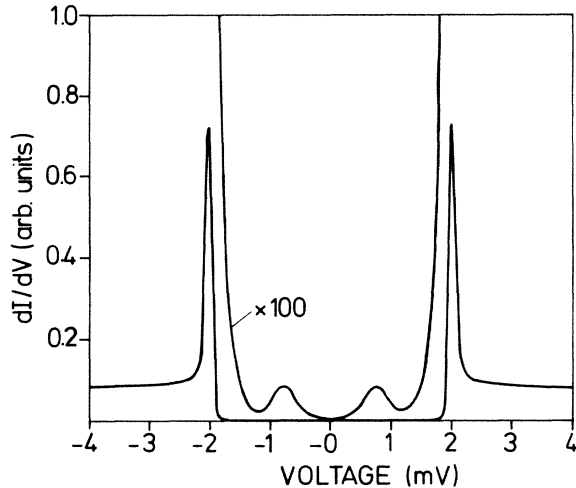


FIG. 1. dI/dV trace of a ZrN/ZrN-oxide/In junction taken at 1.2 K with both electrodes in the superconducting state.

($\Delta_{\text{In}} = 0.53$ meV). Compared with similar measurements taken on $A15$ superconductors⁵ these results indicate an excellent homogeneity of the ZrN film with respect to its superconducting properties. Also, x-ray diffraction measurements showed only sharp lines of the $B1$ phase with a lattice parameter of 0.458 nm. The best films had residual resistivity ratios of 4 and residual resistivities ρ_0 around $4 \mu\Omega$ cm. From Fig. 1 we deduce an energy gap of 1.47 meV for this ZrN film. The energy gap was found to open near 9.2 K, giving a value of 3.7 for $2\Delta_0/kT_c$. The amplified dI/dV trace in Fig. 1 demonstrates the excellently low excess currents and the structures expected at $\Delta_{\text{ZrN}} - \Delta_{\text{In}}$ if both electrodes are superconducting.

In Fig. 2 we show dI/dV data taken in the normal and superconducting states up to a voltage of -120 mV. These are the "raw data" of the tunneling experiments. For all the diodes the background varied more slowly for a negative bias at the ZrN film with respect to the counterelectrode. Therefore the negative polarity was best suited for the measurements. In the superconducting trace near voltages of -20 and -30 mV we clearly see typical resonancelike phonon-induced structures. According to the phonon dispersion data measured by Christensen *et al.*,⁶ these structures are due to the transverse and longitudinal acoustic phonons. In Fig. 2 we further observe a small resonance at about -60 mV. In the phonon dispersion data the optical phonons are located just at this energy. In order to demonstrate the phonon-induced structures more clearly we present in Fig. 3 second-derivative data ($-d^2V/dI^2$) taken in the normal and superconducting states at negative bias. Peaks in the superconducting trace showing upwards are due to peaks or shoulders in the Eliashberg function $\alpha^2(\omega)F(\omega)$. We observe the peaks at -22 and -29 mV which correspond to the energy where the transverse and

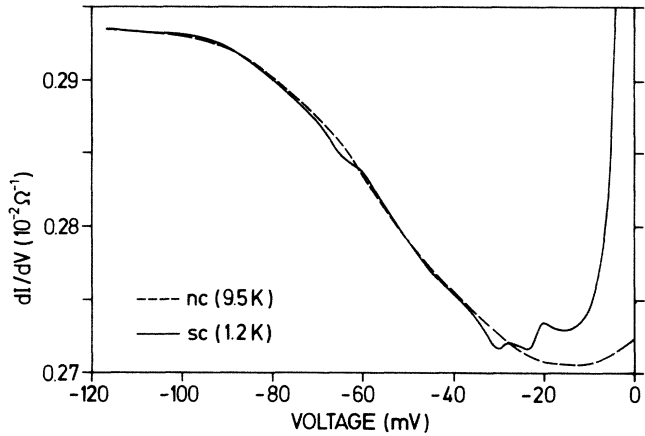


FIG. 2. Derivative measurements (dI/dV vs V) of a ZrN/ZrN-oxide/In tunnel junction taken in the superconducting (solid line) and normal state (dashed line) at negative polarity of the ZrN electrode with respect to the In electrode. The superconductivity of the In electrode has been suppressed by a magnetic field of 0.06 T.

longitudinal acoustic-phonon branches approach the Brillouin zone.⁶ The peak ranging from -60 to -65 mV covers the energy band of the optical phonons. The splitting of this peak into a double-peak structure was observed on all junctions and it can be possibly explained by the splitting of transverse and longitudinal optical phonons.⁶ In Ref. 3 it was shown that, in cases where inelastic effects [they are manifested in the normal conducting (nc) background of Fig. 3 as broad downwards peaks] are comparable in strength and sharpness to the

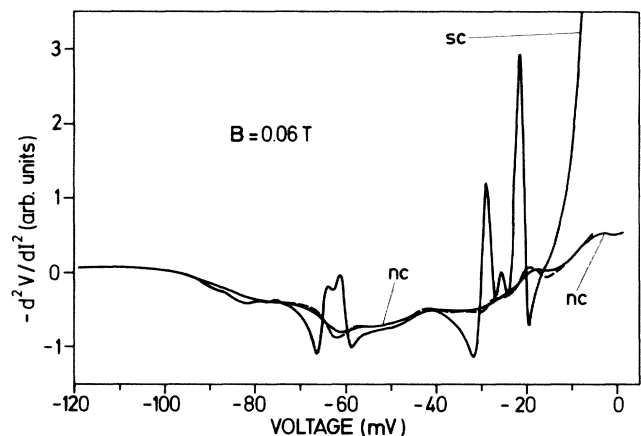


FIG. 3. Second derivative data ($-d^2V/dI^2$) of a ZrN/ZrN-oxide/In tunnel junction taken in the superconducting (sc) and normal (nc) states at negative polarity. Superconductivity in the counterelectrode has been suppressed. Peaks in the sc trace showing upwards are caused by peaks or shoulders in the Eliashberg function. Dashed line: The nc background after correction for temperature smearing and folding with the superconducting density of states.

superconducting structures, the nc background has to be corrected for temperature smearing (the nc background is measured at 9.5 K) and for the influence of the superconducting state on the inelastic structures. In the superconducting state, where in fact the background has to be known, the inelastically scattered electrons decay into the density of states of the superconductor causing a deformation of the inelastic spectrum in the tunnel characteristic. Such corrections have been found² to be of crucial importance in NbN where artificial "optical" peaks may appear at wrong energies^{2,3} (near 47 meV) as compared to phonon data⁷ if the corrections are neglected. The dashed line shows the background corrected in the appropriate way. We notice that in the case of ZrN the correction is of minor importance because of the strong and sharp superconducting structures.

In Fig. 4, we show the results of the McMillan and Rowell (MR) analysis. A straightforward application of the MR program to a RDOS containing a high-energy optical structure leads to instabilities of the iterative procedure at high energies. The calculated data in the upper part of Fig. 4 were obtained in a modified way: First the acoustic and optical parts of the RDOS were analyzed separately. Then both resulting α^2F spectra were combined, and the height of the optical peak was

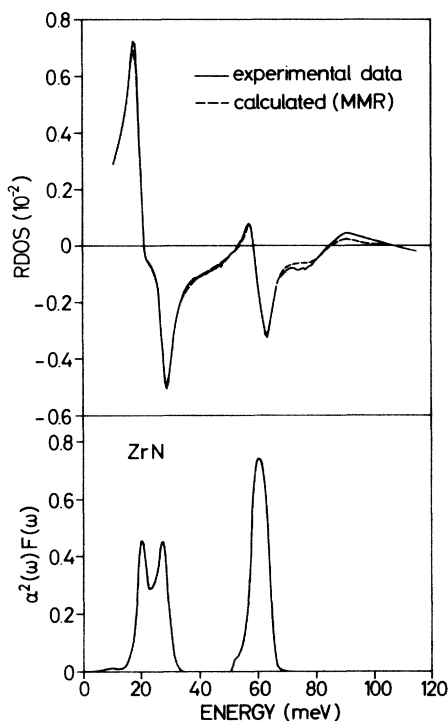


FIG. 4. Upper graph: The measured reduced density of states (RDOS) and the best fit (dashed line) obtained with use of the McMillan-Rowell program as outlined in the text. Lower graph: The resulting Eliashberg function $\alpha^2(\omega)F(\omega)$. The parameters are $\mu^* = 0.10$, $\lambda = 0.62$, $\Delta_0 = 1.46$, $\langle\omega\rangle = 33.2$ meV, $\langle\omega^2\rangle = 1414$ (meV)².

adjusted to get the best fit to the experimental RDOS data. In this way we obtained a remarkably close fit to our data within the classical Eliashberg description as used by the MR program without introducing additional parameters to correct the tunnel data for proximity effects. The resulting α^2F spectrum, composed of an acoustic part ranging to 33 meV and an optical part near 60 meV, is shown in the lower part of Fig. 4. For the Coulomb pseudopotential μ^* we got values near 0.1 for our best junctions, i.e., values within a regime expected for successful tunneling experiments. T_c calculations with these data using the temperature-dependent Eliashberg gap equations yielded a value of 8.4 K. This is in close agreement with the experimental T_c , again indicating the good quality of the tunneling measurements. Speculating on why our ZrN samples yield such good junctions we see two possible explanations. First, there is the exceptional quality of our samples with respect to resistivity ratio and residual resistivity which may result in a comparably high coherence length and thus possibly reduce effects of surface degradation. Second, we found the dynamical conductivity of the junctions up to very high voltages (± 1 V) varying as slowly as that of "classical" Al/Al-oxide/Pb junctions. This indicates that on our films a high and narrow tunnel barrier has formed. So far experience has showed us that such a barrier has a far less degraded interface as compared to a broad and shallow barrier formed typically by Nb oxides.

In Fig. 5 we compare our α^2F result to the result of the theoretical calculation published by Rietschel, Winter, and Reichardt.⁴ These authors applied the rigid-muffin-tin approximation (RMTA) to calculate the α^2F spectra of NbN, VN, ZrN, and TiN. For the phonon frequencies they used the dispersion data of Ref. 6. Excellent agreement is obtained in the positions of the main optical phonon peaks between 59 and 63 meV.

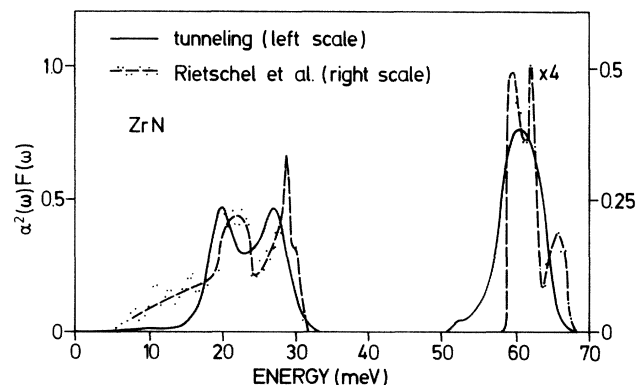


FIG. 5. Comparison of the Eliashberg function resulting from the tunneling experiment (solid line, left scale) and the result of a RMTA calculation (Ref. 4, dots; the broken line serves as a guide to the eye). The optical part of the RMTA result has been reduced before plotting and must be multiplied by 4.

Also in the acoustic region we see that the overall shape of the tunneling data and the theoretical result are similar. The peaks of the tunneling α^2F are shifted by about 2 meV to lower energies. This is probably caused by a difference in composition of the samples. From plots of T_c versus nitrogen content⁸ we deduce the composition of $ZrN_{0.98}$ for our films, whereas the single crystal used by Christensen *et al.*⁶ for the determination of the phonon data had a composition of $ZrN_{0.93}$.

In this paper our main concern is the coupling strength of the optical phonons in comparison to the acoustic phonons which so far has not been determined experimentally. Our tunneling results yield for the ratio of the area of the optical peak to that of the acoustic part of the α^2F spectrum the value of 1.15. This means that the average strength of the electron-phonon coupling function α^2 of the optical phonons is slightly larger than the average acoustical α^2 . This is in contrast to the calculation of Rietschel, Winter, and Reichardt.⁴ Their α^2F shows a ratio of 3.0, thus strongly overestimating the electron-phonon coupling of the optical phonons. This is reflected also in the λ values. The result for the electron-phonon coupling constant λ of Rietschel, Winter, and Reichardt of 0.60 agrees excellently with our result of 0.62. But concerning the different phonon contributions we get $\lambda_{ac}=0.44$ and $\lambda_{opt}=0.18$ whereas Rietschel, Winter, and Reichardt calculate $\lambda_{ac}=\lambda_{opt}=0.3$. It should be emphasized, however, that for the other refractory superconductors treated by Rietschel, Winter, and Reichardt⁴ the ratios $\lambda_{ac}/\lambda_{opt}$ are much closer to our findings for ZrN.

We further remark that on junctions of lower quality, as indicated by reduced μ^* values (for example of 0.06 or 0.04), the ratio of the optical to the acoustical area was still near 1.1. This clearly shows that the junction quality does not change preferentially the intensity of the high-energy phonon-induced structures as has been proposed by Shen⁹ for the case of tunnel junctions on niobium. We think that ZrN is an ideal model system to study such weakening effects, and it is an interesting question whether they occur on junctions with strong proximity effects generated, e.g., by a T_c decrease of the

ZrN film in the vicinity of the tunnel barrier.

In conclusion, we have prepared thin films of ZrN on which nature has provided tunnel barriers with almost ideal properties comparable to the natural tunnel barriers forming on Al films. This enabled us to measure the RDOS up to energies of 120 meV thus including the optical-phonon-induced structures. We could invert our tunnel data using the MR procedure without the need to correct for proximity effects. This means that the superconducting properties of ZrN can be very well described by the classical Eliashberg gap equations. Our most important conclusion is that in ZrN, which we now consider as a model system for tunneling spectroscopy at least in refractory compounds, the optical phonons are coupled to the electrons slightly more strongly than the acoustic phonons.

We thank H. Rietschel, J. M. Rowell, W. Weber, and H. Winter for valuable discussions.

¹J. Geerk, W. Gläser, F. Gompf, W. Reichardt, and E. Schneider, in *Low Temperature Physics-LT 14*, edited by M. Krusius and M. Vuorio (North-Holland, Amsterdam, 1975), Vol. 2, p. 411.

²K. E. Kihlstrom, R. W. Simon, and S. A. Wolf, *Phys. Rev. B* **32**, 1820 (1985).

³J. Geerk, U. Schneider, W. Bangert, H. Rietschel, F. Gompf, M. Gurvitch, R. Remeika, and J. R. Rowell, *Physica* **135B**, 187 (1985).

⁴H. Rietschel, H. Winter, and W. Reichardt, *Phys. Rev. B* **22**, 4284 (1980).

⁵J. Geerk, U. Kaufmann, W. Bangert, and H. Rietschel, *Phys. Rev. B* **33**, 1621 (1986).

⁶A. N. Christensen, O. W. Dietrich, W. Kress, and W. D. Teuchert, *Phys. Rev. B* **19**, 5699 (1979).

⁷A. N. Christensen, O. W. Dietrich, W. Kress, W. D. Teuchert, and R. Currat, *Solid State Commun.* **31**, 795 (1979).

⁸T. Wolf, dissertation, University of Karlsruhe, 1982 (unpublished), p. 26.

⁹L. Y. L. Shen, in *Superconductivity in d- and f-Band Metals*, edited by D. H. Douglass, AIP Conference Proceedings No. 4 (American Institute of Physics, New York, 1972), p. 31.